

An Approximately MAI-Free Multiaccess OFDM System in Carrier Frequency Offset Environment

Shang-Ho Tsai, *Student Member, IEEE*, Yuan-Pei Lin, *Member, IEEE*, and C.-C. Jay Kuo, *Fellow, IEEE*

Abstract—The carrier frequency offset (CFO) effect of a new multiaccess orthogonal frequency division multiplexing (OFDM) transceiver is analyzed. We show that multiaccess interference (MAI) due to CFO can be mitigated by choosing a proper set of orthogonal codes. That is, if we use $M/2$ symmetric or antisymmetric codewords of the M Hadamard–Walsh codewords, MAI can be greatly reduced to a negligible amount. The new OFDM system has been shown to be approximately MAI-free when there is no CFO. The new result developed here shows that the system continues to be approximately MAI-free even in the presence of CFO. Furthermore, we derive a close form for the reduced MAI, which reveals an interesting property of the system. That is, when the number of users increases, the reduced MAI and the inter carrier interference (ICI) due to self-CFO will decrease. Finally, it is demonstrated by simulation that the proposed OFDM scheme with proper code selection outperforms the OFDMA and the multicarrier code division multiplexing access (MC-CDMA) systems in a CFO environment.

Index Terms—Carrier frequency offset (CFO), code selection, frequency synchronization, MAI-free, MC-CDMA, multiuser detection (MUD), multiuser OFDM, OFDMA.

I. INTRODUCTION

MULTICARRIER modulation (MCM) systems have been widely used in both wireline and wireless communications recently [6], [8], [9], e.g., the digital subscriber line (DSL), wireless local area networks (WLANs), and digital video broadcasting (DVB). In wireless environments, MCM systems are usually called orthogonal frequency division multiplexing (OFDM) systems [9]. Due to the mismatch of the oscillators in the transceiver and the Doppler effect, OFDM systems are sensitive to the carrier frequency offset (CFO) effect [18], [20]. The CFO effect will destroy orthogonality of the OFDM systems. Since the loss of orthogonality will lead to significant performance degradation [20], research on accurate CFO estimation and compensation has received a lot of attention in the design of practical OFDM systems [4], [18], [22].

Manuscript received June 10, 2004; revised January 3, 2005. This work was supported in part by the Integrated Media Systems Center, a National Science Foundation Engineering Research Center, under Cooperative Agreement EEC-9529152. Any opinions, findings and conclusions or recommendations expressed in this material are those of the authors and do not necessarily reflect those of the National Science Foundation. The associate editor coordinating the review of this manuscript and approving it for publication was Dr. Behrouz Farhang-Boroujeny.

S.-H. Tsai and C.-C. J. Kuo are with the Department of Electrical Engineering and Integrated Media Systems Center, University of Southern California, Los Angeles, CA 90089-2564 USA. (e-mail: shanghot@usc.edu; cckuo@sipi.usc.edu).

Y.-P. Lin is with the Department of Electrical and Control Engineering, National Chiao Tung University, Hsinchu, Taiwan, R.O.C (e-mail: ypl@mail.nctu.edu.tw).

Digital Object Identifier 10.1109/TSP.2005.857059

The single-user OFDM system has been thoroughly examined in the past, e.g., [6], [8], and [9]. For multiuser OFDM communications, there are two popular techniques; namely, multicarrier code division multiplexing access (MC-CDMA) and orthogonal frequency division multiple access (OFDMA). When compared with CDMA systems, MC-CDMA systems inherit the advantages of multicarrier systems in combating the inter symbol interference (ISI) caused by frequency selective fading channels. Moreover, MC-CDMA systems can fully exploit the frequency diversity. MC-CDMA systems can be divided into two types [14]. In the first type, one bit is transmitted per time slot. The coming bit is spread into several chips, which are allocated to different subchannels. The number of subchannels equals the number of chips [7], [26]. In the second type, several bits are converted from serial-to-parallel and then each bit is spread into several chips. The chips corresponding to the same bit are allocated to the same subchannel [17]. This one is often called the MC-DS CDMA system. Two more generalized MC-CDMA system was proposed in [1], [13], and [14]. In the first scheme [13], [14], each S/P converted bit is spread into several chips and then each subcarrier is modulated with one chip, where the frequency separation corresponding to each bit is maximized to achieve frequency diversity. In the second scheme [1], similarly, each S/P converted bit is spread into several chips. Then, the chips corresponding to the same symbol are modulated in successive subcarriers. Although MC-CDMA systems spread symbols using orthogonal codes to ensure orthogonality, when used in uplink transmission, i.e., from the mobile station (MS) to the base station (BS), orthogonality may be destroyed at the receiver due to frequency selective fading, thus leading to multiaccess interference (MAI). The MAI problem cannot be solved by increasing the transmit power since increasing the transmit power for one user will also increase the interference for other users. To suppress MAI, sophisticated multiuser detection (MUD) [25] and signal processing techniques have been proposed at the receiver end [10], [12], [14]. Furthermore, due to MAI, the CFO estimation and compensation are much more complicated in MC-CDMA systems [11].

The OFDMA systems [21] are MAI-free when there is no CFO. However, OFDMA systems are sensitive to the CFO effect. Moreover, different CFOs of different users make CFO estimation much more difficult than that in the single user OFDM system due to the following reason. When any user has a nonzero CFO, the CFO not only causes the performance degradation of this particular user (i.e., the self-CFO effect) but also leads to MAI for other users. Therefore, OFDMA systems are no longer MAI-free in a CFO environment. CFO estimation

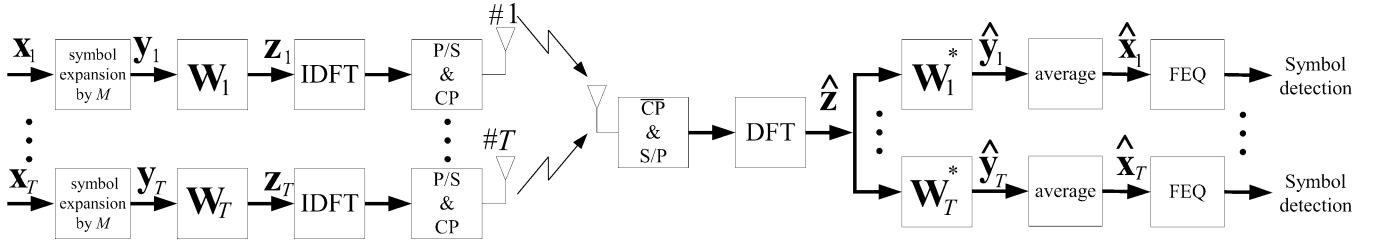


Fig. 1. Block diagram of the proposed system.

algorithms for OFDMA systems were proposed in [2], [5], [19]. However, all those methods demand extra computational complexity in the receiver end. Moreover, CFO compensation needs to be done in the transmitter part so that a feedback mechanism is demanded in this situation [5], [19].

An approximately MAI-free multiaccess OFDM transceiver was proposed in [23]. In this system, every user can utilize the whole bandwidth and time slots simultaneously. When the number of subchannels is sufficiently large in an environment without CFO, the proposed system has the approximately MAI-free property. Unlike the conventional MC-CDMA systems, there is no need to suppress MAI in the receiver, and the system performance improves as the transmit power increases. Moreover, this new system is robust to timing mismatch among users so that it can be conveniently used in uplink transmission [23].

In this work, we first evaluate the CFO effect of the new multiuser OFDM system and derive analytical results for MAI caused by CFO as well as self-CFO impairments. Based on the analytical results, we present a code selection scheme to mitigate MAI by choosing proper orthogonal codes. That is, if we use only the $M/2$ symmetric or the $M/2$ antisymmetric codewords of the M Hadamard–Walsh codes, MAI can be greatly reduced to a negligible amount. Using this code selection, we can reduce MAI caused by CFO without additional complexity such as MUD or complicated signal processing techniques. Once MAI is greatly reduced, the self-CFO impairment can be easily estimated and then compensated using methods developed for the single user OFDM system, e.g., [4], [18], and [22]. Since MAI is reduced to a negligible amount, we can compensate the CFO effect at the receiver end without the feedback. Furthermore, we derive a close form for the reduced MAI with code selection, which reveals an interesting property of the proposed system. That is, when the number of users increases, both the averaged reduced MAI due to others' CFOs and the averaged inter carrier interference (ICI) due to self-CFO will decrease. Finally, it is demonstrated by computer simulation that the proposed system with proper code selection has less MAI and a smaller bit error probability than the OFDMA and the MC-CDMA systems in a CFO environment. The superiority of the proposed system in MAI reduction not only facilitates the CFO estimation task but also improves the system performance.

The rest of this paper is organized as follows. The multiuser OFDM system and its main properties are given in Section II. The MAI effect caused by other users' CFOs, and the self-CFO impairment are analyzed in Section III. Moreover, we derive an close form for the reduced MAI and the self-CFO impairment.

Simulation results are given in Section IV to corroborate the analytical results. Furthermore, performance comparison between the proposed system, the OFDMA, and the MC-CDMA systems is given. Finally, a conclusion is drawn in Section V.

II. SYSTEM MODEL AND ITS PROPERTIES

In this section, we give a brief review of the new OFDM system and its properties [23]. The block diagram of the proposed system in the uplink direction is shown in Fig. 1, where T is the number of users. Let the input of the i th user ($1 \leq i \leq T$) be an $N \times 1$ vector \mathbf{x}_i , which contains N modulation symbols. As shown in Fig. 1, the transmitter consists of four stages. At the first stage, each symbol in vector \mathbf{x}_i is repeated M times to form a new vector \mathbf{y}_i of size $NM \times 1$ as

$$y_i[m + kM] = x_i[k], \quad 0 \leq k \leq N - 1 \text{ and } 0 \leq m \leq M - 1. \quad (1)$$

At the second stage, \mathbf{y}_i is passed through an $NM \times NM$ diagonal matrix \mathbf{W}_i with its diagonal elements drawn from an $M \times M$ unitary matrix \mathbf{D} ($\mathbf{D}^\dagger \mathbf{D} = \mathbf{M}\mathbf{I}$), where the notation \mathbf{D}^\dagger denotes conjugate-transpose of \mathbf{D} . Let the column vectors of \mathbf{D} be $\mathbf{d}_1, \mathbf{d}_2, \dots, \mathbf{d}_M$. Then, \mathbf{W}_i is obtained by repeating \mathbf{d}_i N times along the diagonal, i.e.,

$$\mathbf{W}_i = \text{diag}(\mathbf{d}_i^t \mathbf{d}_i^t \dots \mathbf{d}_i^t)$$

where \mathbf{d}_i^t is the transpose of \mathbf{d}_i . Let $w_i[l]$ be the l th diagonal element of \mathbf{W}_i , $0 \leq l \leq NM - 1$. As $\mathbf{D}^\dagger \mathbf{D} = \mathbf{M}\mathbf{I}$, these diagonal elements satisfy the following property:

$$\sum_{m=0}^{M-1} w_i[m + kM] w_j^*[m + kM] = \begin{cases} M, & i = j \\ 0, & i \neq j \end{cases} \quad (2)$$

where w^* is the conjugate of w , $0 \leq m \leq M - 1$, and $0 \leq k \leq N - 1$. For $M = 2^n$, $n \geq 1$, one sequence that satisfies the condition in (2) is the Hadamard–Walsh code [25]. After passing through the diagonal matrix, the l th component of the $NM \times 1$ orthogonally coded output vector \mathbf{z}_i is given by

$$z_i[l] = w_i[l] y_i[l], \quad 0 \leq l \leq NM - 1. \quad (3)$$

At the third stage, each coded vector is passed through the NM -point unitary inverse discrete Fourier transform (IDFT) matrix. Finally, at the fourth stage, each transformed vector is converted from the parallel to the serial representation and the cyclic prefix (CP) of length ν is added, where ν is the maximum channel delay spread.

At the receiver side, the receiver removes the CP and passes each block of size NM through the unitary discrete Fourier transform (DFT) matrix. For the detection of the symbols transmitted by the i th user, the DFT output vector is multiplied by

\mathbf{W}_i^* and then averaged. Let $\hat{\mathbf{y}}_i$ be the output of \mathbf{W}_i^* and $\hat{\mathbf{x}}_i$ be the averaged output. Then, the k th element of $\hat{\mathbf{x}}_i$ is given by

$$\begin{aligned}\hat{x}_i[k] &= \frac{1}{M} \sum_{m=0}^{M-1} \hat{y}_i[m+kM] \\ &= \frac{1}{M} \sum_{m=0}^{M-1} \hat{z}[m+kM] w_i^*[m+kM], \quad 0 \leq k \leq N-1.\end{aligned}\quad (4)$$

In the final stage, $\hat{\mathbf{x}}_i$ is passed through frequency equalization (FEQ) and ready for detection.

The new multiuser OFDM system has the approximately MAI-free property, which is described as follows [23]. Let $\lambda_i[l]$ be the l th element of the NM -point DFT of channel path i , and let \mathbf{e} be the DFT of the received noise vector of size $NM \times 1$. The l th element of $\hat{\mathbf{z}}$ is given by [6], [8]

$$\hat{z}[l] = \sum_{i=1}^T \lambda_i[l] z_i[l] + e[l], \quad 0 \leq l \leq NM-1. \quad (5)$$

From (3) and (5), the l th element of $\hat{\mathbf{y}}_j$ can be expressed as

$$\hat{y}_j[l] = \sum_{i=1}^T \lambda_i[l] y_i[l] w_i[l] w_j^*[l] + e[l] w_j^*[l]. \quad (6)$$

Let $l = m + kM$. From (4) and (6), the k th element of $\hat{\mathbf{x}}_j$ is given by

$$\begin{aligned}\hat{x}_j[k] &= \frac{1}{M} \sum_{m=0}^{M-1} \lambda_j[m+kM] y_j[m+kM] w_j[m+kM] w_j^*[m+kM] \\ &\quad + \frac{1}{M} \sum_{i=1, i \neq j}^T \sum_{m=0}^{M-1} \lambda_i[m+kM] y_i[m+kM] w_i[m+kM] w_j^*[m+kM] \\ &\quad + \frac{1}{M} \sum_{m=0}^{M-1} e[m+kM] w_j^*[m+kM]\end{aligned}\quad (7)$$

where the second term in (7) is the MAI from other users. When N is sufficiently large, we can approximate $\lambda_i[m+kM]$ by

$$\lambda_i[m+kM] \approx \lambda_i^{(N)}[k], \quad 0 \leq m \leq M-1, \quad 0 \leq k \leq N-1 \quad (8)$$

where $\lambda_i^{(N)}[k]$ is the k th component of the N -point DFT of the i th channel path. The approximation in (8) is also used in [6], [8]. Using (1) and (8), we can rewrite (7) as

$$\begin{aligned}\hat{x}_j[k] &\approx \lambda_j^{(N)}[k] x_j[k] \frac{1}{M} \sum_{m=0}^{M-1} w_j[m+kM] w_j^*[m+kM] \\ &\quad + \frac{1}{M} \sum_{i=1, i \neq j}^T \lambda_i^{(N)}[k] x_i[k] \sum_{m=0}^{M-1} w_i[m+kM] w_j^*[m+kM] \\ &\quad + \frac{1}{M} \sum_{m=0}^{M-1} e[m+kM] w_j^*[m+kM] \\ &= \lambda_j^{(N)}[k] x_j[k] + \frac{1}{M} \sum_{m=0}^{M-1} e[m+kM] w_j^*[m+kM] \quad [\text{by (2)}].\end{aligned}\quad (9)$$

Observed from (9), the MAI is approximately zero. Hence, if there is no channel noise, we can approximately reconstruct $x_i[k]$ by multiplying $\hat{x}_i[k]$ by $(\lambda_i^{(N)}[k])^{-1}$. An alternative for reconstruction is multiplying $\hat{x}_i[k]$ by $((1/M) \sum_{m=0}^{M-1} \lambda_i[m+kM])^{-1}$. Note that the alternative one will lead to more accurate approximation and, hence, better performance. The one-tap gain multiplication is what usually called frequency equalization. Since the proposed system is approximately MAI-free, its capacity increases as SNR increases. This result is very different from that of conventional MC-CDMA systems, in which increasing the transmit power of one user will also increase the MAI for other users.

Although the proposed system uses orthogonal codes such as the Hadamard–Walsh code to distinguish individual users. It is worthwhile to point out several differences between the proposed system and other systems.

A. MAI-Free

The proposed system can achieve approximately MAI-free when N is much larger than the multipath length ν . That is, for a fixed ν , as N increases, the system will have less MAI. Hence, by increasing N , the system can accommodate more users with negligible MAI. This MAI-free property is similar to that of the OFDMA system, which is MAI-free when time and frequency are well synchronized. Moreover, in an OFDMA system, the block duration is in general much longer than the multipath length. Such systems are usually used in wireless local area network (WLAN) applications [16]. On the other hand, CDMA or MC-CDMA systems are usually used in the cellular phone system, where co-channel interference is the major concern. Due to MAI, the number of users accommodated by MC-CDMA systems is much less than the spreading factor M [1], [13], [14]. To increase the number of active users, M should be increased accordingly. This is different from the proposed system where N is increased to achieve both MAI-free and higher loading.

B. Frequency Equalization

Referring to Fig. 1, the proposed system performs “frequency equalization” [8] instead of “combing” before symbol detection. This stands in contrast with MC-CDMA systems, where “combing” is usually used before detection [1], [13], [14]. There are several different combing methods such as MRC, EGC and ORC in MC-CDMA systems [14]. The combing techniques multiply every spread chips by a weighted gain and then sum up every M chips before detection. Hence, there are NM gain multiplications for the MC-CDMA systems [1], [13], [14]. Moreover, due to MAI, multiuser detection may be involved and thus the detection of individual symbols is not independent [14]. On the other hand, from (4), the proposed system performs summation before the gain multiplication, i.e., frequency equalization. Thus, we only need N gain multiplications in the proposed system. Furthermore, since the proposed system is approximately MAI-free, there is no need to use MUD. Thus, the detection for individual symbols is independent.

C. Hadamard–Walsh Code in the Uplink Transmission

In the uplink transmission, it is difficult to guarantee that every user transmits his/her signal simultaneously. This will lead to timing mismatch among users. If the Hadamard–Walsh code is used in the uplink transmission in conventional CDMA systems, a small timing mismatch among users will result in great MAI even if the channel is perfect. For instance, consider the case with processing gain $M = 4$. If the fourth user has a delay of one chip duration while the other three users are perfectly synchronized, the receiver cannot distinguish the fourth user from the third one because $d_4[m-1] = d_3[m]$. Therefore, Hadamard–Walsh code is seldom used in the uplink transmission unless the timing mismatch problem can be well resolved by some other mechanism. In conventional CDMA or MC-CDMA systems, quasiorthogonal codes that have less cross correlation such as the Gold code or the Kasami code are usually used to mitigate the timing mismatch problem. In contrast, since the proposed system is robust to timing mismatch [23], we can adopt the low complexity Hadamard–Walsh code in the uplink transmission.

III. ANALYSIS OF CFO EFFECTS

In the proposed system, the overall CFO effect consists of two parts. One is the MAI caused by CFOs of other users. The other is the symbol distortion and the inter carrier interference (ICI) due to the user's own CFO. They will be analyzed separately in this section.

Consider the l th element of the received vector after DFT in a CFO environment, i.e.,

$$\hat{z}[l] = \sum_{i=1}^T r_i[l] + e[l], \quad 0 \leq l \leq NM - 1 \quad (10)$$

where $r_i[l]$ is the attenuated symbol of $z_i[l]$. The attenuation is caused by channel fading and the CFO effect. Suppose the i th user has a normalized CFO ϵ_i , which is the actual CFO normalized by $1/NM$ of the overall bandwidth and $-0.5 \leq \epsilon_i \leq 0.5$, one can show that $r_i[l]$ in (10) can be expressed by [18]

$$r_i[l] = \underbrace{\alpha_i \lambda_i[l] z_i[l]}_{r_i^{(0)}[l]} + \underbrace{\beta_i \sum_{m=0, m \neq l}^{NM-1} \lambda_i[m] z_i[m] \frac{e^{-j\pi((m-l)/NM)}}{NM \sin \frac{\pi(m-l+\epsilon_i)}{NM}}}_{r_i^{(1)}[l]} \quad (11)$$

where α_i and β_i are given by

$$\alpha_i = \frac{\sin \pi \epsilon_i}{NM \sin \frac{\pi \epsilon_i}{NM}} e^{j\pi \epsilon_i ((NM-1)/NM)}$$

and $\beta_i = \sin(\pi \epsilon_i) e^{j\pi \epsilon_i ((NM-1)/NM)}$. (12)

The first term of (11) is the distorted symbol, and the second term is the ICI caused by the CFO. Note that when there is no CFO, $r_i[l]$ equals $\lambda_i[l] z_i[l]$, as defined in (5). From (4) and (10), we see that $\hat{x}_j[k]$ under CFO is given by

$$\hat{x}_j[k] = \underbrace{\frac{1}{M} \sum_{v=0}^{M-1} r_j[v+kM] w_j^*[v+kM]}_{s_j[k]} + \underbrace{\sum_{i=1, i \neq j}^T \frac{1}{M} \sum_{v=0}^{M-1} r_i[v+kM] w_j^*[v+kM]}_{\text{MAI}_{j \leftarrow i}[k]} + \frac{1}{M} \sum_{v=0}^{M-1} e[v+kM] w_j^*[v+kM] \quad (13)$$

where $\text{MAI}_{j \leftarrow i}[k]$ is the interference due to user i . In the following, $\text{MAI}_{j \leftarrow i}[k]$ and $s_j[k]$ are considered separately.

A. Analysis of Other User's CFO Effect

Let us consider the MAI of the k th symbol of user j due to user i , i.e., $\text{MAI}_{j \leftarrow i}[k]$ in (13). From (11) and (13), we have

$$\text{MAI}_{j \leftarrow i}[k] = A_{j \leftarrow i}[k] + B_{j \leftarrow i}[k] \quad (14)$$

where

$$A_{j \leftarrow i}[k] = \frac{1}{M} \sum_{v=0}^{M-1} r_i^{(0)}[v+kM] w_j^*[v+kM] \quad (15)$$

and

$$B_{j \leftarrow i}[k] = \frac{1}{M} \sum_{v=0}^{M-1} r_i^{(1)}[v+kM] w_j^*[v+kM]. \quad (16)$$

Using (1), (3), and the approximation in (8), we have

$$A_{j \leftarrow i}[k] \approx \frac{\alpha_i}{M} \lambda_i^{(N)}[k] x_i[k] \sum_{v=0}^{M-1} w_i[v+kM] w_j^*[v+kM] = 0. \quad (\text{by (2)}). \quad (17)$$

Therefore, the interference term $A_{j \leftarrow i}[k]$ is approximately zero. Hence, only the term $B_{j \leftarrow i}[k]$ is of concern. The term $B_{j \leftarrow i}[k]$ can be rearranged as (18), shown at the bottom of the page. Letting $m = u + fM$, (18) can be manipulated as (19), shown at the bottom of the next page. Using (1) and the approximation in (8), we have (20), shown at the bottom of the next page. We argue that the term of $f = k$ is the dominating MAI in (20). Since $u \neq v + (k-f)M$, we have

$$\min_{u,v,k,f} \left| \sin \frac{\pi(u-v+(k-f)M+\epsilon_i)}{NM} \right| = \begin{cases} \sin \frac{\pi(-1+\epsilon_i)}{NM}, & \epsilon_i > 0 \\ \sin \frac{\pi(1+\epsilon_i)}{NM}, & \epsilon_i < 0 \end{cases}.$$

$$B_{j \leftarrow i}[k] = \frac{\beta_i}{M} \sum_{v=0}^{M-1} \sum_{m=0, m \neq v+kM}^{NM-1} \lambda_i[m] y_i[m] \frac{e^{-j\pi((m-v-kM)/NM)}}{NM \sin \frac{\pi(m-v-kM+\epsilon_i)}{NM}} w_i[m] w_j^*[v]. \quad (18)$$

When $f = k$, there are $M - 1$ pairs of (u, v) to make the sine function in (20) equal $\sin \pi(1 + \epsilon_i)/NM$ and $M - 1$ pairs of (u, v) to make the sine function equal $\sin \pi(-1 + \epsilon_i)/NM$. On the other hand, when $f = k + 1$ or $f = k - 1$, both situations have only one pair of (u, v) that makes the sine function equal $\sin \pi(1 + \epsilon_i)/NM$ and one pair of (u, v) that makes the sine function equal $\sin \pi(-1 + \epsilon_i)/NM$. Hence, the MAI term of $f = k$ contributes the most to (20). If we can find ways to reduce the term of $f = k$, the MAI can be greatly reduced. Intuitively speaking, the MAI in the k th symbol of the target user is most seriously affected by the k th symbols of other users. The farther the distance of other users' symbols from the k th symbol, the less impact they will make. Later, we will give an example (i.e., Example 3 in Section IV) to illustrate this point.

Since the MAI term of $f = k$ in (20) is the dominating MAI, we will rearrange this term to a form that helps us gain insights on how to reduce it. Let us extract the MAI term of $f = k$ in (20) and let it be denoted by $B_{j \leftarrow i}^{(0)}[k]$, we have

$$B_{j \leftarrow i}[k] = B_{j \leftarrow i}^{(0)}[k] + B_{j \leftarrow i}^{(1)}[k] \quad (21)$$

where

$$B_{j \leftarrow i}^{(0)}[k] \approx \frac{\beta_i}{M} \lambda_i^{(N)}[k] x_i[k] \cdot \sum_{v=0}^{M-1} \sum_{u=0, u \neq v}^{M-1} \frac{e^{-j\pi((u-v)/NM)}}{NM \sin \frac{\pi(u-v+\epsilon_i)}{NM}} w_i[u] w_j^*[v] \quad (22)$$

and

$$B_{j \leftarrow i}^{(1)}[k] = B_{j \leftarrow i}[k] - B_{j \leftarrow i}^{(0)}[k]. \quad (23)$$

Referring to (22), let

$$g(p) = e^{-j\pi p/NM} / NM \sin(\pi(p + \epsilon_i)/NM), \quad - (M - 1) \leq p \leq M - 1, p \neq 0.$$

When N is sufficiently large, the denominator of $g(p)$ is approximately an odd function of p , and the numerator is nearly

constant for all possible p with $-M + 1 \leq p \leq M - 1, p \neq 0$. Hence, we can approximate $g(p)$ as an odd function of p , i.e., $g(p) \approx -g(-p)$. Using the equality shown at the bottom of the page, and the approximation $g(p) \approx -g(-p)$, we can rewrite (22) as

$$B_{j \leftarrow i}^{(0)}[k] \approx \frac{\beta_i}{M} \lambda_i^{(N)}[k] x_i[k] \cdot \sum_{p=1}^{M-1} g(p) \underbrace{\sum_{q=0}^{M-1-p} \{w_i[p+q] w_j^*[q] - w_i[q] w_j^*[p+q]\}}_{\mathcal{O}}. \quad (24)$$

As given in (24), the quantity \mathcal{O} is determined by the property of orthogonal codewords. If $\mathcal{O} = 0$, the dominating MAI term of $f = k$ in (20) is approximately zero. One way to achieve this is the use of only $M/2$ of the M Hadamard–Walsh codes, which are either symmetric or antisymmetric.

Proposition: Suppose only the $M/2$ symmetric or the $M/2$ antisymmetric codewords of the M Hadamard–Walsh codes are used, $\mathcal{O} = 0$, and thus, $B_{j \leftarrow i}^{(0)}[k] \approx 0$.

Proof: The M Hadamard–Walsh code can be divided into two groups of $M/2$ codewords [15]. One is the set of symmetric (even) codes satisfying

$$w_i[l] = w_i[M - 1 - l], \quad 0 \leq l \leq \frac{M}{2} - 1 \quad (25)$$

and the other is the set of antisymmetric (odd) codes given by

$$w_i[l] = -w_i[M - 1 - l], \quad 0 \leq l \leq \frac{M}{2} - 1. \quad (26)$$

When symmetric codewords are used, from (25) and since Hadamard–Walsh code is real, we have

$$\begin{aligned} & \sum_{q=0}^{M-1-p} w_i[p+q] w_j^*[q] \\ &= \sum_{q=0}^{M-1-p} w_i[M - 1 - (p+q)] w_j[M - 1 - q]. \end{aligned} \quad (27)$$

$$B_{j \leftarrow i}[k] = \frac{\beta_i}{M} \sum_{v=0}^{M-1} \sum_{f=0}^{N-1} \sum_{u=0, u \neq v+(k-f)M}^{M-1} \lambda_i[u+fM] y_i[u+fM] \cdot \frac{e^{-j\pi((u-v-(k-f)M)/NM)}}{NM \sin \frac{\pi(u-v-(k-f)M+\epsilon_i)}{NM}} w_i[u] w_j^*[v]. \quad (19)$$

$$B_{j \leftarrow i}[k] \approx \frac{\beta_i}{M} \sum_{f=0}^{N-1} \lambda_i^{(N)}[f] x_i[f] \sum_{v=0}^{M-1} \sum_{u=0, u \neq v+(k-f)M}^{M-1} \frac{e^{-j\pi((u-v-(k-f)M)/NM)}}{NM \sin \frac{\pi(u-v-(k-f)M+\epsilon_i)}{NM}} w_i[u] w_j^*[v]. \quad (20)$$

$$\sum_{v=0}^{M-1} \sum_{u=0, u \neq v}^{M-1} g(u-v) w_i[u] w_j^*[v] = \sum_{p=1}^{M-1} \left\{ g(p) \sum_{q=0}^{M-1-p} w_i[p+q] w_j^*[q] + g(-p) \sum_{q=0}^{M-1-p} w_i[q] w_j^*[p+q] \right\}$$

Let $q' = M - 1 - p - q$. We can rewrite (27) as

$$\begin{aligned} \sum_{q=0}^{M-1-p} w_i[p+q]w_j^*[q] &= \sum_{q'=M-1-p}^0 w_i[q']w_j[p+q'] \\ &= \sum_{q=0}^{M-1-p} w_i[q]w_j^*[p+q]. \end{aligned} \quad (28)$$

Thus, \mathcal{O} in (24) is zero. As for the set of antisymmetric codewords, from (26), we again have the same equality as given in (27). This leads to (28). Therefore, the use of antisymmetric codewords also results in $\mathcal{O} = 0$. ■

Let us give a simple example for codeword selection [24]. Suppose $M = 8$ and \mathbf{D}_8 is an 8×8 Hadamard matrix with column vectors $\mathbf{d}_1, \mathbf{d}_2, \dots, \mathbf{d}_8$. We can either choose column vectors $\{\mathbf{d}_1, \mathbf{d}_4, \mathbf{d}_6, \mathbf{d}_7\}$, which are symmetric, or column vectors $\{\mathbf{d}_2, \mathbf{d}_3, \mathbf{d}_5, \mathbf{d}_8\}$, which are antisymmetric, as the four codewords for four users.

If the proposed code selection is used, the dominating MAI $B_{j \leftarrow i}^{(0)}[k]$ can be reduced to a negligible amount. Therefore, the MAI terms of $f \neq k$ in (23) become the main MAI impairment. For convenience, with code selection, let us call it residual MAI. Next, we will investigate the residual MAI. From (20) and (22), we have (29), shown at the bottom of the page. Let $l = f - k$. For fixed k , $-k \leq l \leq N - 1 - k$ and $l \neq 0$, (29) can be rewritten as (30), shown at the bottom of the page. Letting $f(p, l) = e^{-j\pi p/NM} / NM \sin(\pi(p + lM + \epsilon_i)/NM)$, we

have (31), shown at the bottom of the page. Using (28) and (31), we can rewrite (30), as shown in (32) at the bottom of the page. Assume that $\lambda_i^{(N)}[k]$ and $x_i[k]$ are uncorrelated for all k , and $x_i[k]$ and $x_i[k']$ are uncorrelated for $k \neq k'$. From the Appendix, it can be shown that the expectation value for the mean square of $B_{j \leftarrow i}^{(1)}[k]$ is

$$\begin{aligned} E \left\{ \left| B_{j \leftarrow i}^{(1)}[k] \right|^2 \right\} &\approx \frac{|\beta_i|^2}{M^2} \sigma_{\lambda_i}^2 \sigma_{x_i}^2 \\ &\cdot \sum_{l=1}^{N-1} \left| \sum_{p=1}^{M-1} [f(p, l) + f(-p, l)] \sum_{q=0}^{M-1-p} w_i[q]w_j^*[p+q] \right|^2 \end{aligned} \quad (33)$$

where $\sigma_{\lambda_i}^2$ is the averaged channel gain, and $\sigma_{x_i}^2$ is the averaged symbol power of user i defined by

$$\sigma_{\lambda_i}^2 = E \left\{ \left| \lambda_i^{(N)}[k] \right|^2 \right\} \text{ and } \sigma_{x_i}^2 = E \left\{ |x_i[k]|^2 \right\}, \quad 0 \leq k \leq N-1. \quad (34)$$

Example 1: Assume $\sigma_{\lambda_i}^2 = \sigma_{x_i}^2 = 1$. Let us first consider the CFO case of $\epsilon_i = 0.3$. This CFO level may be regarded as a serious one. Let $M = 16$ and $N = 4$. Fig. 2 shows the total residual MAI, i.e., $\sum_{i=1, i \neq j}^T E \left\{ \left| B_{j \leftarrow i}^{(1)}[k] \right|^2 \right\}$, as a function of the user index, where the summation term accounts for $T = M/2$ users in this system. As shown in Fig. 2, the worst total residual MAI is about -18.5 dB, which is much smaller than the transmit power of 0 dB. Since the residual MAI

$$B_{j \leftarrow i}^{(1)}[k] \approx \frac{\beta_i}{M} \sum_{f=0, f \neq k}^{N-1} \lambda_i^{(N)}[f] x_i[f] \sum_{v=0}^{M-1} \sum_{u=0}^{M-1} \frac{e^{-j\pi((u-v-(k-f)M)/NM)}}{NM \sin \frac{\pi(u-v-(k-f)M+\epsilon_i)}{NM}} w_i[u]w_j^*[v]. \quad (29)$$

$$B_{j \leftarrow i}^{(1)}[k] \approx \frac{\beta_i}{M} \sum_{l=-k, l \neq 0}^{N-1-k} \lambda_i^{(N)}[k+l] x_i[k+l] \underbrace{\sum_{v=0}^{M-1} \sum_{u=0}^{M-1} \frac{e^{-j\pi((u-v+lM)/NM)}}{NM \sin \frac{\pi(u-v+lM+\epsilon_i)}{NM}} w_i[u]w_j^*[v]}_{\zeta}. \quad (30)$$

$$\begin{aligned} \zeta &= e^{-j\pi l/N} \sum_{v=0}^{M-1} \sum_{u=0}^{M-1} f(u-v, l) w_i[u]w_j^*[v] \\ &= e^{-j\pi l/N} \sum_{p=1}^{M-1} \left\{ f(p, l) \sum_{q=0}^{M-1-p} w_i[p+q]w_j^*[q] + f(-p, l) \sum_{q=0}^{M-1-p} w_i[q]w_j^*[p+q] \right\}. \end{aligned} \quad (31)$$

$$B_{j \leftarrow i}^{(1)}[k] \approx \frac{\beta_i}{M} \sum_{l=-k, l \neq 0}^{N-1-k} e^{-j\pi l/N} \lambda_i^{(N)}[k+l] x_i[k+l] \sum_{p=1}^{M-1} [f(p, l) + f(-p, l)] \sum_{q=0}^{M-1-p} w_i[q]w_j^*[p+q]. \quad (32)$$

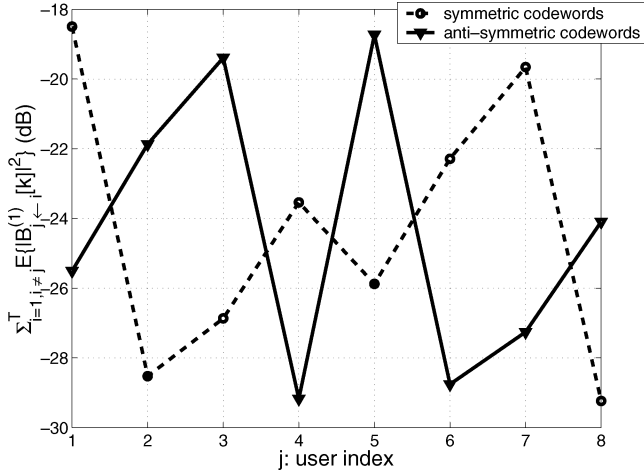


Fig. 2. Example 1: $\sum_{i=1, i \neq j}^T E \left\{ \left| B_{j \leftarrow i}^{(1)}[k] \right|^2 \right\}$ as a function of user index j with $M = 16$ for symmetric and antisymmetric codewords.

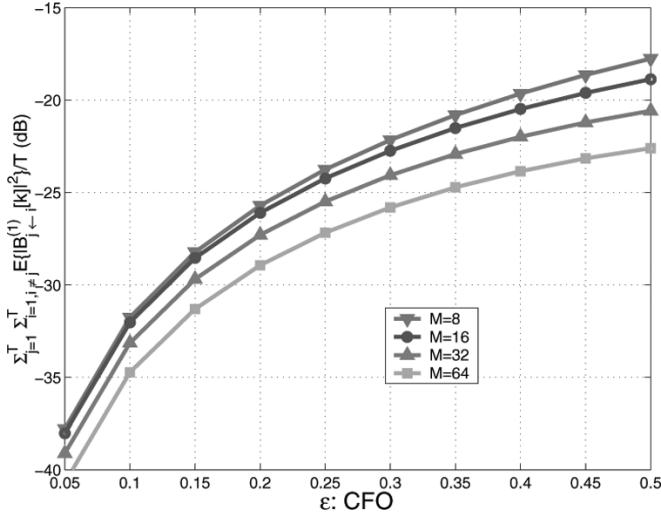


Fig. 3. Example 1: $(1/T) \sum_{j=1}^T \sum_{i=1, i \neq j}^T E \left\{ \left| B_{j \leftarrow i}^{(1)}[k] \right|^2 \right\}$ as a function of CFO for different M .

$B_{j \leftarrow i}^{(1)}[k]$ is relatively small, it will make channel estimation and CFO estimation much more accurate. Let us consider the averaged value of total residual MAI for all users, i.e., $(1/T) \sum_{j=1}^T \sum_{i=1, i \neq j}^T E \left\{ \left| B_{j \leftarrow i}^{(1)}[k] \right|^2 \right\}$. Fig. 3 shows the averaged value of total residual MAI as a function of CFO for different M with symmetric codewords. The performance with antisymmetric codewords is also similar to this figure. From Fig. 3, we see that, as M increases, the averaged total residual MAI decreases. This result means that the increase of M will help reduce $B_{j \leftarrow i}^{(1)}[k]$. Note that since there are $T = M/2$ users in this system, the increase of M will also increase the number of users. It implies that the increase of users can help reduce the residual MAI for a fixed CFO.

Although the codeword selection given in the Proposition decreases the number of users from M to $M/2$, it reduces the dominating MAI greatly and the system is approximately MAI-free in the presence of CFOs. Thus, every user only has to tackle his/her own CFO problem without worrying about the CFOs of other users. This is very different from conventional multiaccess OFDM systems, where sophisticated signal processing is used to solve the multiuser CFO problem [2], [5], [11], [19]. Significant reduction of the dominating MAI using symmetric or antisymmetric codewords will only be verified by experimental results in Section IV.

B. Analysis of Self-CFO Effect

In this subsection, we examine the impairment caused by self-CFO. For user j , the self-CFO impairment means the symbol distortion and the interference caused by his/her own CFO ϵ_j . From (11) and (13), we have

$$s_j[k] = C_j[k] + D_j[k] \quad (35)$$

where $C_j[k]$ is the distorted symbol of $x_j[k]$ due to self-CFO given by

$$\begin{aligned} C_j[k] &= \frac{1}{M} \sum_{v=0}^{M-1} r_j^{(0)}[v + kM] w_j^*[v + kM] \\ &= \frac{\alpha_j}{M} \sum_{v=0}^{M-1} \lambda_j[v + kM] y_j[v + kM] w_j[v + kM] w_j^*[v + kM] \text{ [by (3)]} \\ &\approx \frac{\alpha_j}{M} \lambda_j^{(N)}[k] x_j[k] \sum_{v=0}^{M-1} w_j[v + kM] w_j^*[v + kM] \text{ [by (1) and (8)]} \\ &= \alpha_j \lambda_j^{(N)}[k] x_j[k] \text{ [by (2)]} \end{aligned} \quad (36)$$

and $D_j[k]$ is the interference caused by $x_j[f]$, $0 \leq f \leq N - 1$

$$D_j[k] = \frac{1}{M} \sum_{v=0}^{M-1} r_j^{(1)}[v + kM] w_j^*[v + kM]. \quad (37)$$

Using the same procedure of deriving (16), (18), (19) and (20), we have (38), shown at the bottom of the page.

Using the same procedure of deriving (22) and (24), the term of $f = k$ in (38), which is the interference caused by the k th symbol itself, can be written as

$$\begin{aligned} D_j^{(0)}[k] &\approx \frac{\beta_j}{M} \lambda_j^{(N)}[k] x_j[k] \\ &\cdot \sum_{p=1}^{M-1} g(p) \underbrace{\sum_{q=0}^{M-1-p} \{w_j[p+q] w_j^*[q] - w_j[q] w_j^*[p+q]\}}_{\mathcal{O}'} \\ &= 0 \end{aligned} \quad (39)$$

where $\mathcal{O}' = 0$ because $w_j[m] = w_j[m + kM]$, $0 \leq m \leq M - 1$ and $0 \leq k \leq N - 1$. Therefore, we have $D_j^{(0)}[k] \approx 0$.

$$D_j[k] \approx \frac{\beta_j}{M} \sum_{f=0}^{N-1} \lambda_j^{(N)}[f] x_j[f] \sum_{v=0}^{M-1} \sum_{u=0, u \neq v + (k-f)M}^{M-1} \frac{e^{-j\pi((u-v-(k-f)M)/NM)}}{NM \sin \frac{\pi(u-v-(k-f)M + \epsilon_j)}{NM}} w_j[u] w_j^*[v]. \quad (38)$$

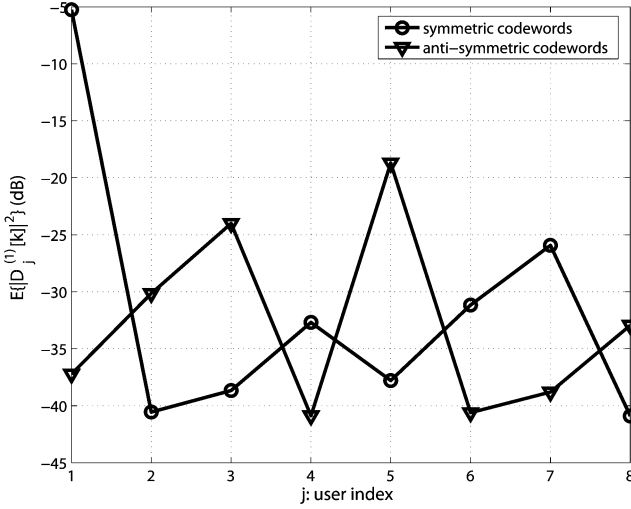


Fig. 4. Example 2: $E \left\{ \left| D_{j \leftarrow i}^{(1)}[k] \right|^2 \right\}$ as a function of user index j with $M = 16$ for symmetric and antisymmetric codewords.

Next, consider the terms of $f \neq k$ in (38), which is the ICI caused by all other symbols except for the k th symbols. Using the same procedure of deriving (29) to (32), we have (40), shown at the bottom of the page. From the derivation in the Appendix, (40) can be shown to be

$$E \left\{ \left| D_j^{(1)}[k] \right|^2 \right\} \approx \frac{|\beta_j|^2}{M^2} \sigma_{\lambda_j}^2 \sigma_{x_j}^2 \cdot \sum_{l=1}^{N-1} \left| \sum_{p=1}^{M-1} [f(p,l) + f(-p,l)] \sum_{q=0}^{M-1-p} w_j[q] w_j^*[p+q] + M f(0,l) \right|^2. \quad (41)$$

Example 2: The environment setting is the same as that stated in Example 1. First, let us consider the averaged ICI $E \left\{ \left| D_j^{(1)}[k] \right|^2 \right\}$ for each individual user, which is plotted as a function of user index in Fig. 4. We see that the worst performance is around -6 dB for the user with codeword \mathbf{d}_1 , i.e., the all-one code. Other codewords have performance smaller than -17 dB. The reason for \mathbf{d}_1 to yield significantly large ICI can be given as follows.

For convenience, let us repeat the definition of $f(p,l)$, i.e., $f(p,l) = e^{-j\pi p/NM} / NM \sin(\pi(p+lM+\epsilon_i)/NM)$ in reference to (41). The denominator of $f(p,l)$ is positive for all possible l and p , whereas its numerator can be approximated by 1 for all p when N is sufficiently large. Thus, $f(p,l)$ is positive approximately. A similar argument can be applied to $f(-p,l)$ as well. For the all-one code, $\sum_{q=0}^{M-1-p} w_1[q] w_1^*[p+q] = (M-p)$ is positive for all p . Together with the fact that both

$f(p,l)$ and $f(-p,l)$ are positive approximately, we conclude that the all-one code results in a much larger value in $\left| \sum_{p=1}^{M-1} [f(p,l) + f(-p,l)] \sum_{q=0}^{M-1-p} w_j[q] w_j^*[p+q] \right|^2$ than other codewords, whose $\sum_{q=0}^{M-1-p} w_j[q] w_j^*[p+q]$ can be either negative or positive.

Since the ICI using all other symmetric codewords are below -27 dB (except \mathbf{d}_1), this result suggests the use of symmetric codewords but excluding the all-one code to have a smaller ICI. According to (36), the distorted symbol due to self-CFO has the mean square expectation value given by $E \left\{ |C_j[k]|^2 \right\} = -1.3$ dB when $|\epsilon_j| = 0.3$ and $\sigma_{\lambda_i}^2 = \sigma_{x_i}^2 = 1$. Except \mathbf{d}_1 , the amount $E \left\{ \left| D_j^{(1)}[k] \right|^2 \right\}$ of other users is much smaller than -1.3 dB. Moreover, when compared with the residual MAI that is below -18 dB in Example 1, the -1.3 dB of the distorted symbol is still relatively large as compared with the residual MAI. Since the residual MAI and ICI are both smaller than the distorted symbol due to the self-CFO, we can estimate α_j accurately and compensate it in the receiver end without demanding a feedback mechanism. We will discuss this in more detail in the next section. The averaged ICI for all users as a function of CFO for different M , i.e., $(1/T) \sum_{j=1}^T E \left\{ \left| D_j^{(1)}[k] \right|^2 \right\}$, is shown in Fig. 5. Since \mathbf{d}_1 is excluded, there are $M/2 - 1$ users in the system with symmetric codewords. We see that symmetric codewords with \mathbf{d}_1 excluded have a smaller averaged ICI than antisymmetric codewords. From the figure, we see results similar to Fig. 3. That is, the increase of M helps reduce ICI for a fixed CFO. Note that for target user j , the ICI due to self-CFO ϵ_j only affects itself. Even if \mathbf{d}_1 is included for symmetric codewords, it does not result in significant performance degradation for other users since the MAI caused by \mathbf{d}_1 to all other users is sufficiently small according to the discussion in Section III-A.

C. Overall CFO Estimation and Compensation

Here, let us consider the overall CFO effect. For convenience, let us rewrite (13) as

$$\hat{x}_j[k] \approx \alpha_j \lambda_j^{(N)} [k] x_j[k] + \underbrace{D_j[k]}_{\text{self-CFO interference}} + \underbrace{\sum_{i=1, i \neq j}^T \text{MAI}_{j \leftarrow i}[k]}_{\text{MAI from other users}} + \underbrace{\frac{1}{M} \sum_{m=0}^{M-1} e^{j\pi(m+kM)/NM} w_j^*[m]}_{\text{additive noise}}. \quad (42)$$

Following the discussion in Sections III-A and B, impairments due to MAI and self-CFO interference are negligible if only $M/2$ symmetric or antisymmetric codewords of the M Hadamard-Walsh codes are used. The first term of (42)

$$D_j^{(1)}[k] \approx \frac{\beta_j}{M} \sum_{l=0-k, l \neq 0}^{N-1-k} e^{-j\pi l/N} \lambda_j^{(N)} [k+l] x_j[k+l] \cdot \left\{ \sum_{p=1}^{M-1} [f(p,l) + f(-p,l)] \sum_{q=0}^{M-1-p} w_j[q] w_j^*[p+q] + f(0,l) \sum_{q=0}^{M-1} w_j[q] w_j^*[q] \right\}. \quad (40)$$

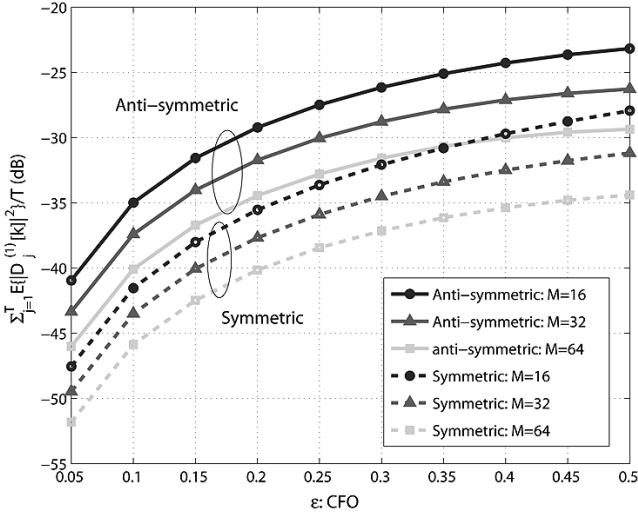


Fig. 5. Example 2: $(1/T) \sum_{i=1, i \neq j}^T E \left\{ |D_{j \leftarrow i}^{(1)}[k]|^2 \right\}$ as a function of CFO for different M , where the all-one code is excluded for the set of symmetric codewords.

is much larger than all other terms (with the exception of the all-one code whose self-CFO interference term is not too small according to Example 2). Thus, we can estimate α_j accurately and compensate it before the detection stage (i.e., every symbol multiplies α_j^{-1} before detection). The alternative is to estimate self-CFO ϵ_j of each user accurately with algorithms for single-user OFDM systems, as developed in [4], [18], and [22]. Once ϵ_j is estimated, we can multiply the l th received symbols of user j by $e^{j2\pi(-l\epsilon_j)/NM}$ to remove the self-CFO effect before passing them through the DFT matrix. The penalty is that a separate DFT is needed for each user. Note that this alternative can be used to estimate ϵ_1 of the all-one code.

In this case, sophisticated MUD techniques and the feedback mechanism are not needed at the receiver end. On the other hand, if the MAI is not reduced, the CFO estimation for each user could be difficult and MUD techniques are needed, which imposes a heavy computational burden on the receiver. For example, CFOs of other users will cause the MAI to any target user in OFDMA systems and signal processing techniques are often used to estimate the CFO of this target user [2], [5], [19]. Furthermore, since OFDMA does not have a negligible MAI-free property in the CFO environment, the feedback mechanism is demanded after CFO estimation so that every user can compensate his/her own CFO at the transmitter end [5].

IV. SIMULATION RESULTS

In this section, we perform computer simulation to corroborate the theoretical results derived in previous sections. Moreover, we will compare the performance of the proposed system, the OFDMA systems and two MC-CDMA systems under the CFO environment. We consider the performance in the uplink direction so that every user has different CFO and channel fading. We assume the channel and the CFO are quasiinvariant in the sense that it remains unchanged within one block duration. Simulations are conducted with the following parameter setting throughout this section. $M = 16$, and the binary phase-shift keying (BPSK) modulation is used. The

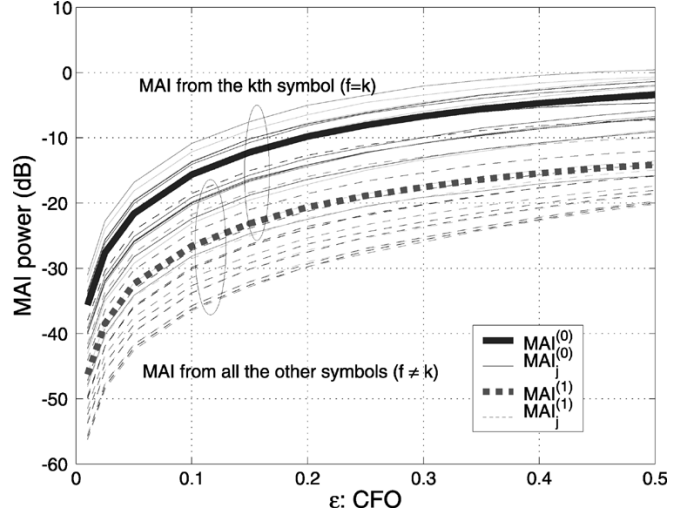


Fig. 6. Example 3: MAI effect as a function of the CFO when the full M Hadamard–Walsh codewords are used.

channel coefficients are independently identically distributed (i.i.d.) complex Gaussian random variables with a unit variance. For every individual user, the Monte Carlo method is used to run more than 500 000 symbols. We consider the worst CFO situation. That is, the CFO value of each user is randomly assigned to be either $+\epsilon$ or $-\epsilon$.

Example 3—Suppression of Dominating MAI Term: Here, we would like to show that $B_{j \leftarrow i}^{(0)}[k]$ defined in (22) is the dominating MAI term in (20), and it can be greatly reduced using only $M/2$ symmetric or antisymmetric codewords of the M Hadamard–Walsh codewords. Let channel be flat and $N = 4$. Then, $A_{j \leftarrow i}[k] = 0$ and $\text{MAI}_{j \leftarrow i}[k] = B_{j \leftarrow i}[k]$ according to (14) and (17), where exact equalities are due to flat channel. Using similar notation rule in (21), we define the MAI from the k th symbol of user i to user j as $\text{MAI}_{j \leftarrow i}^{(0)}[k]$, and the MAI from all the other symbols of user i as $\text{MAI}_{j \leftarrow i}^{(1)}[k]$, i.e., $\text{MAI}_{j \leftarrow i}^{(1)}[k] = \text{MAI}_{j \leftarrow i}[k] - \text{MAI}_{j \leftarrow i}^{(0)}[k]$. Let the number of users $T = M = 16$, i.e., a fully loaded system. The total MAI for user j from the k th symbol of all other users, which is denoted by $\overline{\text{MAI}}_j^{(0)}$, is calculated as follows. For the k th symbol of a target user, we accumulate the MAI contributed from the k th symbol of other 15 users. The procedure is repeated, and then, the MAI power is averaged for k from 0 to $N - 1$. That is, $\overline{\text{MAI}}_j^{(0)}$ is obtained by averaging the value $(1/N) \sum_{k=0}^{N-1} \left| \sum_{i=1, i \neq j}^T \text{MAI}_{j \leftarrow i}^{(0)}[k] \right|^2$ for more than 500 000 symbols. Similarly, the total MAI from all the other symbols ($f \neq k$) of all the other users, which is denoted by $\overline{\text{MAI}}_j^{(1)}$, is obtained by averaging the value, $(1/N) \sum_{k=0}^{N-1} \left| \sum_{i=1, i \neq j}^T \text{MAI}_{j \leftarrow i}^{(1)}[k] \right|^2$, for more than 500 000 symbols.

The total MAI is plotted as a function of the normalized CFO value in Fig. 6, where $\overline{\text{MAI}}_j^{(0)}$ and $\overline{\text{MAI}}_j^{(1)}$ of 16 users are shown by 16 solid and 16 dashed curves, respectively. The solid bold curve in Fig. 6, which is denoted by $\overline{\text{MAI}}^{(0)}$, is the averaged value of the 16 solid curves. That is, $\overline{\text{MAI}}^{(0)}$ is obtained via $(1/T) \sum_{j=1}^T \overline{\text{MAI}}_j^{(0)}$. Similarly, the dashed bold curve, which

is denoted by $\overline{\text{MAI}}^{(1)}$, is obtained by averaging the 16 dashed curves. That is, $\overline{\text{MAI}}^{(1)}$ is obtained via $(1/T) \sum_{j=1}^T \overline{\text{MAI}}_j^{(1)}$. From this figure, we see that $\overline{\text{MAI}}^{(0)}$ is around 10–11 dB more than that of $\overline{\text{MAI}}^{(1)}$. Hence, for each user, the MAI at the k th symbol is mostly contributed from the k th symbols of other users. Thus, it confirms the derived theoretical result that $B_{j \leftarrow i}^{(0)}[k]$ in (22) is the dominating MAI in (20). In the following, we call $B_{j \leftarrow i}^{(0)}[k]$ “dominating MAI” and $B_{j \leftarrow i}^{(1)}[k]$ “residual MAI” for short.

Next, we demonstrate that the dominating MAI can be greatly reduced using only $M/2$ symmetric codewords of the M Hadamard–Walsh codes. Let the user number decreases from $T = M = 16$ to $T = M/2 = 8$, and only the $M/2 = 8$ symmetric codewords are used. The performance is shown in Fig. 7(a). Compared with Fig. 6, the residual MAI decreases around 4 to 5 dB due to the number of users decreasing from 16 to 8. In contrast, the dominating MAI is greatly reduced by 12–47 dB. Note that, the simulation result of the residual MAI is consistent with the theoretical result in Fig. 3. Moreover, we see that using symmetric codewords, the dominating MAI is even smaller than that of the residual MAI when the CFO is less than 0.35.

The performance using $M/2$ antisymmetric codewords is shown in Fig. 7(b). Compared with Fig. 7(a), we see that the performance of the set of antisymmetric codewords is similar to that of the set of symmetric codewords. The result confirms that the dominating MAI can be greatly reduced using the proposed code selection scheme.

Example 4—Comparison of CFO Effect on the Proposed System, OFDMA and MC-CDMA: Here, we would like to compare the CFO effect on the proposed system, the OFDMA system, and two MC-CDMA systems over a flat channel. Among the two MC-CDMA schemes, one is with subcarriers uniformly allocated (called MC-CDMA/U for short) [13], [14], whereas the other is with subcarriers successively allocated (called MC-CDMA/S for short) [1]. Every user in these four systems will transmit N symbols, and the DFT/IDFT size is the same, i.e., NM . Since all four systems transmit N symbols per block and add the CP of the same length ν , their actual data rates are the same. We consider both fully loaded and half-loaded situations. In a fully loaded situation, the Hadamard–Walsh code is used in the proposed and the two MC-CDMA systems. For OFDMA, each user occupies N subchannels which are maximally separated [21], i.e., user u will be assigned subchannels indexed by $(u - 1) + kM$, $1 \leq u \leq M$ and $0 \leq k \leq N - 1$. In a half-loaded case, $M/2$ symmetric codewords of the Hadamard–Walsh code (code selection scheme) are used in the proposed system and the two MC-CDMA systems. For OFDMA, the u th user will be assigned subchannels indexed by $2(u - 1) + kM$, $1 \leq u \leq M/2$ and $0 \leq k \leq N - 1$. The remaining $NM/2$ subchannels are used as guard bands.

Let us first evaluate the MAI in the detection stage, i.e., MAI after frequency equalization. In the absence of MAI and channel noise, the received symbols for detection are still BPSK symbols with either $+1$ or -1 . For the proposed system and the OFDMA

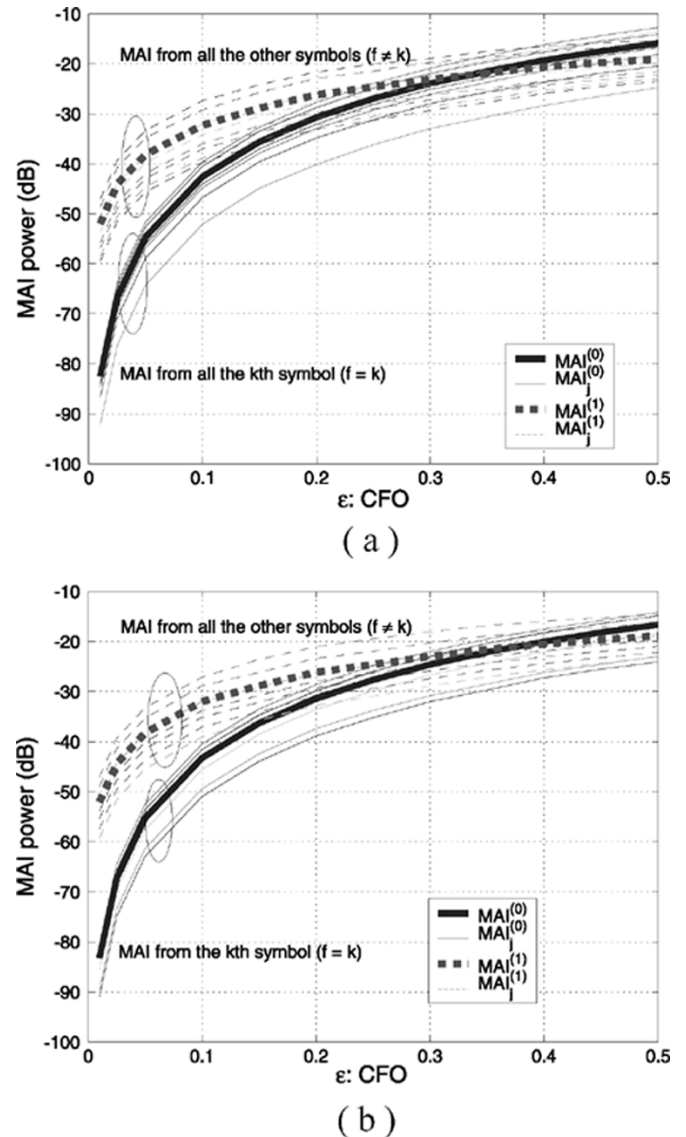


Fig. 7. Example 3: MAI effect as a function of the CFO (a) when only $M/2$ symmetric Hadamard–Walsh codewords are used and (b) when only $M/2$ antisymmetric Hadamard–Walsh codewords are used.

system, frequency equalization was discussed in Section II. For the two MC-CDMA systems, the orthogonality restoring combing (ORC) scheme is used to achieve equalization [14]. To distinguish from the MAI before equalization, we denote the MAI after equalization by $\text{MAI}'_{j \leftarrow i}[k]$. For instance, in the proposed system, $\text{MAI}'_{j \leftarrow i}[k] = \text{MAI}_{j \leftarrow i}[k]/\lambda_j^{(N)}[k]$. The averaged total MAI after equalization is obtained via averaging the value $(1/T) \sum_{j=1}^T (1/N) \sum_{k=0}^{N-1} \left| \sum_{i=1, i \neq j}^T \text{MAI}'_{j \leftarrow i}[k] \right|^2$ for 500,000T symbols. Fig. 8 shows the averaged total MAI after equalization as a function of CFO for the four systems in fully loaded and half-loaded situations. Note that the performance of the proposed system and the MC-CDMA/S are the same for the flat channel; therefore, the two curves overlapped. In the fully loaded case, the MC-CDMA/U outperforms all other three systems. When the number of users decreases from 16 to 8, the MAI of the proposed system is greatly reduced by 15 to 16 dB,

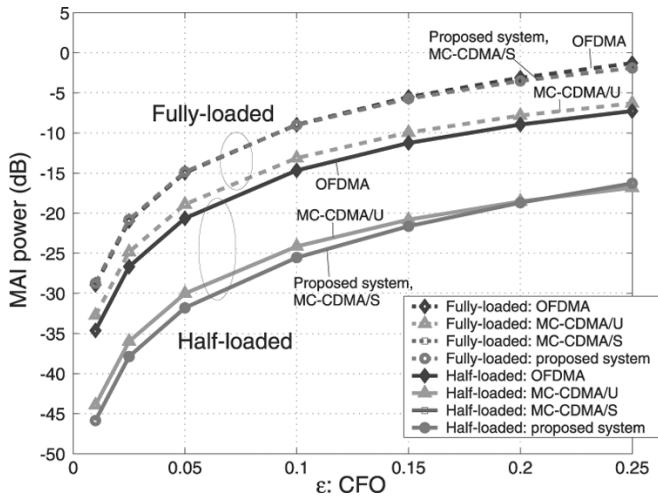


Fig. 8. Example 4: MAI comparison among the proposed system, the OFDMA system, and two MC-CDMA systems in a flat-fading environment.

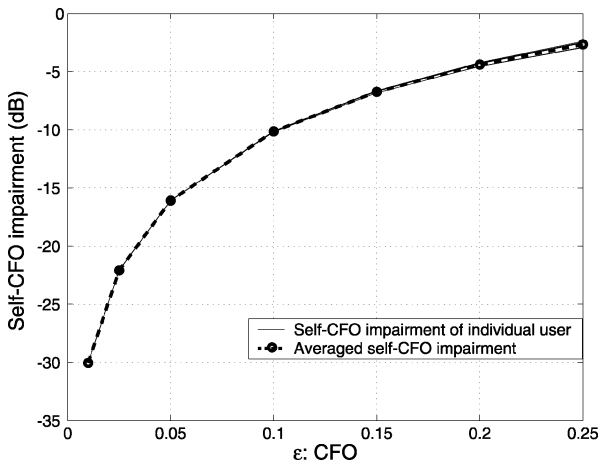


Fig. 9. Example 4: Self-CFO impairment of the proposed system.

and consequently, the proposed system outperforms OFDMA by 10 to 11 dB. Recall that in Example 1, the dominating MAI of the proposed system is larger than the residual MAI by around 10 to 11 dB in the fully loaded situation. Using code selection, the dominating MAI is reduced to a amount that is even smaller than the residual MAI. This explains why the proposed system has similar performance with OFDMA in a fully loaded situation, whereas it outperforms OFDMA by 10 to 11 dB in a half-loaded situation with code selection.

The self-CFO impairment of the proposed system with symmetric codewords is shown in Fig. 9. To compute the self-CFO impairment after frequency equalization, we accumulate the symbol distortion and the interference for the k th symbol of a target user due to his/her own CFO. This procedure is repeated, and then, the impairment power is averaged for k , $0 \leq k \leq N - 1$. The self-CFO impairment of the eight users in the proposed system are indicated by the eight solid curves in Fig. 9. Since the self-CFO impairment of an individual user is similar, these curves are overlapping. The bold-circled curve in Fig. 9 is the averaged value of the eight solid curves. By comparing this figure with Fig. 8, we see that the self-CFO impairment is the main impairment in the proposed system.

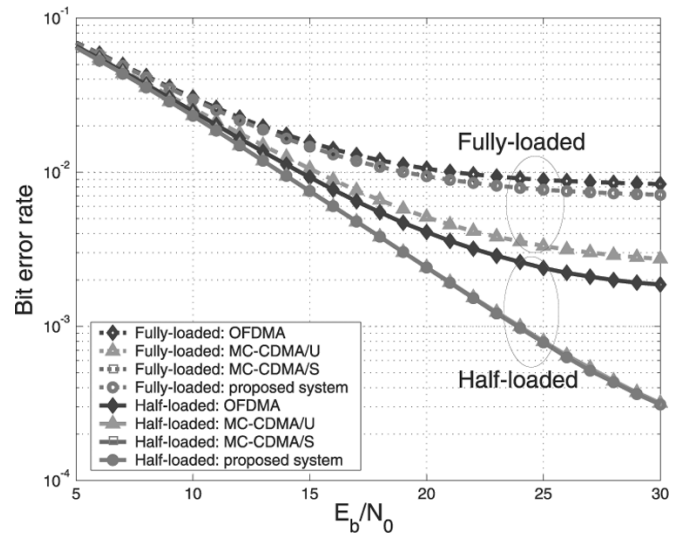


Fig. 10. Example 4: BER comparison among the proposed system, OFDMA, and two MC-CDMA systems in a flat channel with a normalized CFO $|\epsilon_j| = 0.1$.

Since the MAI is relatively small, we can estimate α_j or ϵ_j accurately and then compensate the self-CFO effect, as discussed in Section III-C. It is worthwhile to point out that, although not shown here, the self-CFO impairment of OFDMA is very similar to that given in this figure.

Now, assume that each user has a normalized CFO of $|\epsilon_j| = 0.1$ and can accurately estimate the self-CFO in these four systems. We would like to find out the bit error rate (BER) when there is no feedback. The BERs for the four systems are shown in Fig. 10. For a fully loaded situation, the BER curves of the proposed system and MC-CDMA/S are overlapping. Moreover, for a half-loaded situation, the BER curves of the proposed system MC-CDMA/S and MC-CDMA/U are overlapping. We see that the BER performance has a similar trend as that of the MAI performance in Fig. 8.

Example 5—CFO Effect in a Multipath Environment: In this example, we examine the CFO effect when the channel has the multipath frequency-selective fading. The number of multipath is assumed to be $\nu = 4$ and $N = 64$, whereas the other parameters remain the same as those given in Example 4. The MAI performance of the four systems is shown in Fig. 11. In a fully loaded situation with the CFO smaller than 0.05, OFDMA has less MAI than the proposed system because OFDMA is completely MAI-free when frequency and time are well synchronized. However, as CFO grows, the proposed system slightly outperforms OFDMA system. In a half-loaded situation, the proposed system outperforms OFDMA by around 10 dB due to the use of the code selection. The low MAI value of the proposed system with code selection is also beneficial to CFO estimation.

Let us see the comparison with MC-CDMA. The MAI performance curves for the two MC-CDMA systems with ORC are not good since ORC amplifies the MAI power in the subcarrier with serious fading [14]. In a multipath environment, it is likely that the frequency selective fading contains several zeros to cause huge MAI in the two MC-CDMA systems. However, since a large MAI value may only lead to the error of certain bits, MAI may not be a good performance measure for this case. Instead,

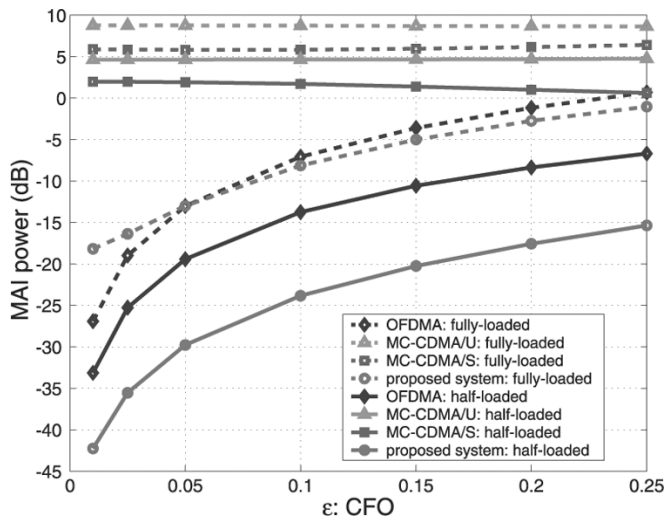


Fig. 11. Example 5: MAI comparison among the proposed system, the OFDMA system, and two MC-CDMA systems in a multipath fading environment.

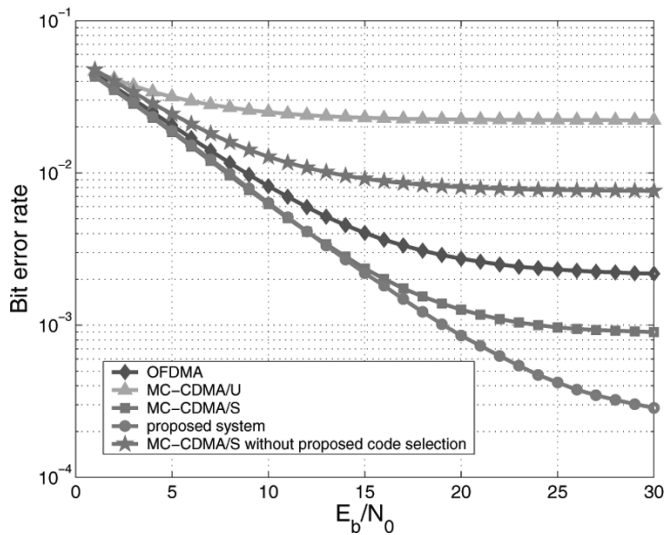


Fig. 12. Example 5: BER comparison among the proposed system, OFDMA, and two MC-CDMA systems with $\nu = 4$ and $|\epsilon_j| = 0.1$ in a half-loaded situation.

the BER may provide a more valuable measure for fair comparison. As MC-CDMA systems with MRC outperform those with ORC in a multipath environment, we will use MRC for the two MC-CDMA systems in the following discussion.

Fig. 12 shows the BER comparison among the four systems with $|\epsilon_j| = 0.1$ in a half-loaded situation. We see that MC-CDMA/S with the proposed code selection outperforms OFDMA. Note that if the code selection is not used in MC-CDMA/S, instead, e.g., the first $M/2$ codewords of the M Hadamard-Walsh code are used, the performance as shown in the star curve is much worse than that using code selection. This result shows the advantage of using code selection in certain conventional MC-CDMA system. Furthermore, although the half-loaded MC-CDMA/U has the worst performance in a multipath environment, this scheme can achieve a better frequency diversity order and can perform better when the number of users

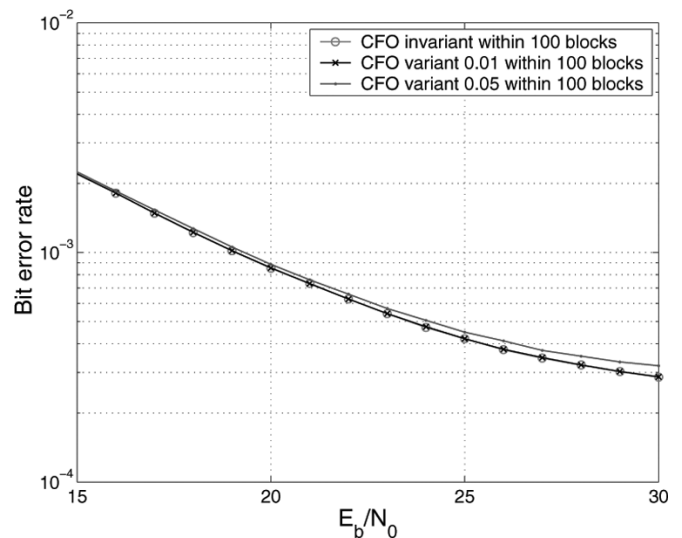


Fig. 13. Example 6: BER performance as a function of SNR in the presence of changing CFO within one OFDM block.

is small [13]. Finally, we observe that the proposed system with code selection outperforms OFDMA and the two MC-CDMA systems in a half-loaded situation with multipath fading.

Example 6—Fast Variant CFO Environment: In this example, we consider a situation when CFO changes so rapidly that its value varies even within one OFDM block. Let the parameters remain the same as those in Example 5. We assume that the system estimates CFO per 100 blocks. We simulate three cases. The first case is that the CFO does not change within 100 blocks. The second one is that the CFO changes ± 0.01 within 100 blocks, e.g., from 0.1 to 0.1 ± 0.01 or from -0.1 to -0.1 ± 0.01 during 100 blocks. The step size is $\pm 0.01/(100(NM + \nu))$ per sample in the transmitted block of size $NM + \nu$. The third one is that the CFO changes ± 0.05 within 100 blocks. Due to the CFO variation, there is a discrepancy between the actual CFO and the estimated CFO. We want to evaluate the impairment due to this discrepancy. It is worthwhile to point out the CFO changing rate in the second and third cases are much larger than that in today's practical operating environment. Thus, they provide extreme difficult cases to test the performance of the proposed system. For instance, let the OFDM-block duration be $256 \mu\text{s}$, carrier frequency be 4 GHz, and the mobile speed be equal to 100 km/h [16], [19]. The normalized CFO can be calculated to be around 0.09 when $NM = 1024$. If the distance between mobile station and base station is 0.02 km, the maximum normalized CFO changing rate is around ± 0.003 per 100 OFDM blocks.

The circled curve of Fig. 13 shows the BER performance for case 1. Since the CFO does not change within 100 blocks, this curve is the same as the circled curve in Fig. 12. The cross curve shows the BER performance for case 2, where the CFO changes $\pm 10\%$ within 100 blocks. We see that the results of cases 1 and 2 are close. Finally, the dotted curve gives the BER performance for case 3, where CFO changes $\pm 50\%$ within 100 blocks. We observe only minor BER degradation in such a fast CFO-changing environment.

V. CONCLUSION

The CFO effect of an approximately MAI-free multiaccess OFDM transceiver was studied in this paper. We showed analytically that the MAI due to CFO can be greatly reduced using either the $M/2$ symmetric or the $M/2$ antisymmetric codewords of the M Hadamard–Walsh codes in the system. As a result, it does not demand sophisticated MUD or signal processing in achieving multiuser communications, and CFO compensation can be done at the receiver side. It was demonstrated by computer simulation that the proposed OFDM scheme has a much better performance than the OFDMA and the MC-CDMA systems in a CFO environment.

 APPENDIX
 PROOF (33)

Suppose that $x_i[k]$ and $\lambda_i^{(N)}[k]$ are uncorrelated. From (32), we have (43), shown at the bottom of the page. Since

we assume the crosscorrelation between $x_i[k]$ is zero, i.e., $E\{x_i[k+l]x_i^*[k+l']\} = 0$ for $l \neq l'$, we can rewrite (43) as

$$\begin{aligned} & E\left\{\left|B_{j \leftarrow i}^{(1)}[k]\right|^2\right\} \\ &= \frac{|\beta_i|^2}{M^2} \sum_{l=-k, l \neq 0}^{N-1-k} E\left\{\left|\lambda_i^{(N)}[k+l]\right|^2\right\} E\left\{|x_i[k+l]|^2\right\} \\ & \cdot \left|\sum_{p=1}^{M-1} [f(p, l) + f(-p, l)] \sum_{q=0}^{M-1-p} w_i[q] w_j^*[p+q]\right|^2. \end{aligned} \quad (44)$$

Using the assumption in (34), we have

$$\begin{aligned} & E\left\{\left|B_{j \leftarrow i}^{(1)}[k]\right|^2\right\} = \frac{|\beta_i|^2}{M^2} \sigma_{\lambda_i}^2 \sigma_{x_i}^2 \\ & \cdot \sum_{l=-k, l \neq 0}^{N-1-k} \underbrace{\left|\sum_{p=1}^{M-1} [f(p, l) + f(-p, l)] \sum_{q=0}^{M-1-p} w_i[q] w_j^*[p+q]\right|^2}_{\varphi(l, i, j)}. \end{aligned} \quad (45)$$

$$\begin{aligned} & E\left\{\left|B_{j \leftarrow i}^{(1)}[k]\right|^2\right\} = \frac{|\beta_i|^2}{M^2} E\left\{\sum_{l=-k, l \neq 0}^{N-1-k} \lambda_i^{(N)}[k+l] x_i[k+l] \sum_{p=1}^{M-1} [f(p, l) + f(-p, l)] \sum_{q=0}^{M-1-p} w_i[q] w_j^*[p+q]\right\} \\ & \cdot \left\{\sum_{l'=-k, l' \neq 0}^{N-1-k} \lambda_i^{(N)}[k+l'] x_i[k+l'] \sum_{p=1}^{M-1} [f(p, l') + f(-p, l')] \sum_{q=0}^{M-1-p} w_i[q] w_j^*[p+q]\right\}^* \\ &= \frac{|\beta_i|^2}{M^2} \sum_{l=-k, l \neq 0}^{N-1-k} \sum_{l'=-k, l' \neq 0}^{N-1-k} E\left\{\lambda_i^{(N)}[k+l] \left(\lambda_i^{(N)}[k+l']\right)^* E\{x_i[k+l] x_i^*[k+l']\}\right\} \\ & \cdot \left\{\sum_{p=1}^{M-1} [f(p, l) + f(-p, l)] \sum_{q=0}^{M-1-p} w_i[q] w_j^*[p+q]\right\} \cdot \left\{\sum_{p=1}^{M-1} [f(p, l') + f(-p, l')] \sum_{q=0}^{M-1-p} w_i[q] w_j^*[p+q]\right\}^*. \end{aligned} \quad (43)$$

$$\begin{aligned} & \sum_{l=-k}^{-1} \left|\sum_{p=1}^{M-1} [f(p, l) + f(-p, l)] \sum_{q=0}^{M-1-p} w_i[q] w_j^*[p+q]\right|^2 \\ &= \sum_{l'=N-k}^{N-1} \left|\sum_{p=1}^{M-1} \left[\frac{e^{-j\pi p/NM}}{NM \sin \frac{\pi(p+(l'-N)M+\epsilon_i)}{NM}} + \frac{e^{j\pi p/NM}}{NM \sin \frac{\pi(-p+(l'-N)M+\epsilon_i)}{NM}}\right] \sum_{q=0}^{M-1-p} w_i[q] w_j^*[p+q]\right|^2 \\ &= \sum_{l'=N-k}^{N-1} \left|\sum_{p=1}^{M-1} \left[\frac{-e^{-j\pi p/NM}}{NM \sin \frac{\pi(p+l'M+\epsilon_i)}{NM}} + \frac{-e^{j\pi p/NM}}{NM \sin \frac{\pi(-p+l'M+\epsilon_i)}{NM}}\right] \sum_{q=0}^{M-1-p} w_i[q] w_j^*[p+q]\right|^2 \\ &= \sum_{l'=N-k}^{N-1} \left|\sum_{p=1}^{M-1} \left[\frac{e^{-j\pi p/NM}}{NM \sin \frac{\pi(p+l'M+\epsilon_i)}{NM}} + \frac{e^{j\pi p/NM}}{NM \sin \frac{\pi(-p+l'M+\epsilon_i)}{NM}}\right] \sum_{q=0}^{M-1-p} w_i[q] w_j^*[p+q]\right|^2 \\ &= \sum_{l=N-k}^{N-1} \left|\sum_{p=1}^{M-1} [f(p, l) + f(-p, l)] \sum_{q=0}^{M-1-p} w_i[q] w_j^*[p+q]\right|^2. \end{aligned} \quad (48)$$

Now, we will show the following equality:

$$\sum_{l=-k, l \neq 0}^{N-1-k} \varphi(l, i, j) = \sum_{l=1}^{N-1} \varphi(l, i, j). \quad (46)$$

Using the definition of $f(p, l)$, we have

$$\begin{aligned} & \sum_{l=-k, l \neq 0}^{N-1-k} \varphi(l, i, j) \\ &= \sum_{l=-k}^{-1} \left| \sum_{p=1}^{M-1} [f(p, l) + f(-p, l)] \sum_{q=0}^{M-1-p} w_i[q] w_j^*[p+q] \right|^2 \\ &+ \sum_{l=1}^{N-1-k} \left| \sum_{p=1}^{M-1} [f(p, l) + f(-p, l)] \sum_{q=0}^{M-1-p} w_i[q] w_j^*[p+q] \right|^2. \end{aligned} \quad (47)$$

Letting $l' = N + l$, the first term on the right-hand side of (47) can be manipulated as (48), shown at the bottom of the previous page. From (47) and (48), we can reach (46). Using (46), we can rewrite (45) as in (33). ■

ACKNOWLEDGMENT

The authors would like to thank the anonymous reviewers for their constructive suggestions, which have significantly improved the quality of this work.

REFERENCES

- [1] S. Abeta, H. Atarashi, and M. Sawahashi, "Forward link capacity of coherent DS-CDMA and MC-CDMA broadband packet wireless access in a multi-cell environments," in *Proc. IEEE Veh. Technol. Conf.*, vol. 5, Sep. 2000, pp. 2213–2218.
- [2] S. Barbarossa, M. Pompili, and G. B. Giannakis, "Channel-independent synchronization of orthogonal frequency division multiple access systems," *IEEE J. Sel. Areas Commun.*, vol. 20, no. 2, pp. 474–486, Feb. 2002.
- [3] K. G. Beauchamp, *Walsh Functions and Their Applications*. New York: Academic, 1975.
- [4] J.-J. van de Beek, M. Sandell, and P. O. Börjesson, "ML estimation of time and frequency offset in OFDM systems," *IEEE Trans. Signal Processing*, vol. 45, no. 7, pp. 1800–1805, Jul. 1997.
- [5] J. J. van de Beek, P. O. Börjesson, M. L. Boucheret, D. Landström, J. M. Arenas, P. Ödling, C. Östberg, M. Wahlqvist, and S. K. Wilson, "A time and frequency synchronization scheme for multiuser OFDM," *IEEE J. Sel. Areas Commun.*, vol. 17, no. 11, pp. 1900–1914, Nov. 1999.
- [6] J. A. C. Bingham, "Multicarrier modulation for data transmission: An idea whose time has come," *IEEE Commun. Mag.*, vol. 28, no. 5, pp. 5–14, May 1990.
- [7] A. Chouly, A. Brajal, and S. Jourdan, "Orthogonal multicarrier techniques applied to direct sequence spread spectrum CDMA systems," in *Proc. IEEE Globecom*, vol. 3, Dec. 1993, pp. 1723–1728.
- [8] J. S. Chow, J. C. Tu, and J. M. Cioffi, "A discrete multitone transceiver system for HDSL applications," *IEEE J. Sel. Areas Commun.*, vol. 9, no. 8, pp. 895–908, Aug. 1991.
- [9] L. J. Cimini Jr., "Analysis and simulation of a digital mobile channel using orthogonal frequency division multiplexing," *IEEE Trans. Commun.*, vol. 33, no. 7, pp. 665–675, Jul. 1985.
- [10] A. Dekorsy, V. Kühn, and K.-D. Kammeyer, "Exploiting time and frequency diversity by iterative decoding in OFDM-CDMA systems," in *Proc. IEEE Globecom*, vol. 5, Dec. 1999, pp. 2576–2580.
- [11] J. H. Deng and T. S. Lee, "An iterative maximum SINR receiver for multicarrier CDMA systems over a multipath fading channel with frequency offset," *IEEE Trans. Wireless Commun.*, vol. 2, no. 3, pp. 560–569, May 2003.
- [12] L. Fang and L. B. Milstein, "Successive interference cancellation in multicarrier DS/CDMA," *IEEE Trans. Commun.*, vol. 48, no. 7, pp. 1530–1540, Sep. 2000.
- [13] X. Gui and T. S. Ng, "Performance of asynchronous orthogonal multicarrier CDMA system in frequency selective fading channel," *IEEE Trans. Commun.*, vol. 47, no. 7, pp. 1084–1091, Jul. 1999.
- [14] S. Hara and R. Prasad, "Overview of multicarrier CDMA," *IEEE Commun. Mag.*, vol. 35, no. 12, pp. 126–133, Dec. 1997.
- [15] H. F. Harmuth, "Applications of Walsh function in communications," *IEEE Spectrum*, vol. 6, Nov. 1969.
- [16] I. Koffman and V. Roman, "Broadband wireless access solutions based on OFDM access in IEEE 802.16," *IEEE Commun. Mag.*, vol. 40, no. 4, pp. 96–103, Apr. 2002.
- [17] S. Kondo and L. B. Milstein, "Performance of multicarrier DS CDMA systems," *IEEE Trans. Commun.*, vol. 44, no. 2, pp. 238–246, Feb. 1996.
- [18] P. H. Moose, "A technique for orthogonal frequency division multiplexing frequency offset correction," *IEEE Trans. Commun.*, vol. 42, no. 10, pp. 2908–2914, Oct. 1994.
- [19] M. Morelli, "Timing and frequency synchronization for the uplink of an OFDMA system," *IEEE Trans. Commun.*, vol. 52, no. 2, pp. 296–306, Feb. 2004.
- [20] T. Pollet, M. V. Bladel, and M. Moeneclaey, "BER sensitivity of OFDM systems to carrier frequency offset and Wiener phase noise," *IEEE Trans. Commun.*, vol. 43, no. 2/3/4, pp. 191–193, Feb./Mar./Apr. 1995.
- [21] H. Sari, Y. Levy, and G. Karam, "An analysis of orthogonal frequency-division multiple access," in *Proc. IEEE Globecom*, vol. 3, Nov. 1997, pp. 1635–1639.
- [22] T. M. Schmidl and D. C. Cox, "Robust frequency and timing synchronization for OFDM," *IEEE Trans. Commun.*, vol. 45, no. 12, pp. 1613–1621, Dec. 1997.
- [23] S. H. Tsai, Y. P. Lin, and C.-C. J. Kuo, "A repetitively coded multicarrier CDMA (RCMC-CDMA) transceiver for multiuser communications," in *Proc. IEEE Wireless Commun. Networking Conf.*, Mar. 2004.
- [24] —, "Enhanced performance for an approximately MAI-free multiaccess OFDM transceiver by code selection," in *Proc. IEEE Veh. Technol. Conf. Fall*, 2004.
- [25] S. Verdu, *Multisuser Detection*. Cambridge, U.K.: Cambridge Univ. Press, 1998.
- [26] N. Yee, J. P. Linnartz, and G. Fettweis, "Multi-carrier CDMA in indoor wireless radio networks," *IEICE Trans. Commun.*, vol. E77-B, pp. 900–904, Jul. 1994.



Shang-Ho Tsai (S'04) was born in Kaohsiung, Taiwan, R.O.C., in 1973. He received the B.S. degree in electrical engineering from Tamkang University, Taipei, Taiwan, in 1995, the M.S. degree in electrical and control engineering from National Chiao-Tung University, Hsinchu, Taiwan, in 1999, and the Ph.D. degree in electrical engineering from the University of Southern California, Los Angeles, in 2005.

From 1999 to 2002, he was with Silicon Integrated Systems Corp., Taiwan, where he participated the VLSI design for DMT-ADSL systems. His research interests include signal processing for communications, particularly the areas of multicarrier systems and space-time processing.

Dr. Tsai received a government scholarship for overseas study from the Ministry of Education, Taiwan, from 2002 to 2005.



Yuan-Pei Lin (S'93–M'97) was born in Taipei, Taiwan, R.O.C., 1970. She received the B.S. degree in control engineering from the National Chiao-Tung University, Hsinchu, Taiwan, in 1992 and the M.S. and the Ph.D. degrees, both in electrical engineering, from the California Institute of Technology, Pasadena, in 1993 and 1997, respectively.

She joined the Department of Electrical and Control Engineering of National Chiao-Tung University in 1997. Her research interests include digital signal processing, multirate filterbanks, and signal

processing for digital communication, particularly the area of multicarrier transmission.

Dr. Lin is a recipient of the 2004 Ta-You Wu Memorial Award. She is currently an associate editor for *IEEE TRANSACTIONS ON SIGNAL PROCESSING*, the *EURASIP Journal on Applied Signal Processing*, and *Multidimensional Systems and Signal Processing*.



C.-C. Jay Kuo (F'99) received the B.S. degree from the National Taiwan University, Taipei, Taiwan, R.O.C., in 1980 and the M.S. and Ph.D. degrees from the Massachusetts Institute of Technology, Cambridge, in 1985 and 1987, respectively, all in electrical engineering. He is with the Department of Electrical Engineering, the Signal and Image Processing Institute (SIPI), and the Integrated Media Systems Center (IMSC), the University of Southern California (USC), Los Angeles, as Professor of electrical engineering and mathematics. His research

interests are in the areas of digital media processing, multimedia compression, communication and networking technologies, and embedded multimedia system design. He has guided approximately 60 students to their Ph.D. degrees and supervised 15 postdoctoral research fellows. Currently, his research group at USC consists of about 30 Ph.D. students and five postdoctoral students, which is one of the largest academic research groups in multimedia technologies. He is a co-author of more than 700 technical publications in international conferences and journals as well as the following seven books: *Content-based Audio Classification and Retrieval for Audiovisual Data Parsing* with T. Zhang (Boston, MA: Kluwer, 2001), *Semantic Video Object Segmentation for Content-based Multimedia Applications* with J. Guo (Boston, MA: Kluwer, 2001), *Intelligent Systems for Video Analysis and Access Over the Internet* with W. Zhou (Englewood Cliffs, NJ: Prentice-Hall, 2002), *Video Content Analysis Using Multimodal Information* with Y. Li (Boston, MA: Kluwer, 2003), *Quality of Service for Internet Multimedia* with J. Shin and D. Lee (Englewood Cliffs, NJ: Prentice-Hall, 2003), *Radio Resource Management for Multimedia QoS Support in Wireless Cellular Networks* with H. Chen, L. Huang, and S. Kumar (Boston, MA: Kluwer, 2003), and *High Fidelity Multichannel Audio Coding* (with D. T. Yang and C. Kyriakakis (Cairo, Egypt: Hindawi, 2004).

Dr. Kuo is a Fellow of SPIE. He received the National Science Foundation Young Investigator Award (NYI) and Presidential Faculty Fellow (PFF) Award in 1992 and 1993, respectively. He is Editor-in-Chief for the *Journal of Visual Communication and Image Representation*, and Editor for the *Journal of Information Science and Engineering* and the *EURASIP Journal of Applied Signal Processing*. He is also on the Editorial Board of the *IEEE Signal Processing Magazine*. He served as Associate Editor for *IEEE TRANSACTIONS ON IMAGE PROCESSING* from 1995 to 1998, *IEEE TRANSACTIONS ON CIRCUITS AND SYSTEMS FOR VIDEO TECHNOLOGY* from 1995 to 1997, and *IEEE TRANSACTIONS ON SPEECH AND AUDIO PROCESSING* from 2001 to 2003.